

BIOPHYSICAL AND PHENOMENOLOGICAL MODELS OF MULTIPLE SPIKE INTERACTIONS IN SPIKE-TIMING DEPENDENT PLASTICITY

Mathilde Badoual, Quan Zou, Andrew P. Davison, Michael Rudolph,
Thierry Bal, Yves Frégnac and Alain Destexhe

*Integrative and Computational Neuroscience Unit (UNIC), CNRS,
1 Avenue de la Terrasse, 91198 Gif-sur-Yvette, France
E-mail: Destexhe@iaf.cnrs-gif.fr*

Spike-timing dependent plasticity (STDP) is a form of associative synaptic modification which depends on the respective timing of pre- and post-synaptic spikes. The biophysical mechanisms underlying this form of plasticity are currently not known. We present here a biophysical model which captures the characteristics of STDP, such as its frequency dependency, and the effects of spike pair or spike triplet interactions. We also make links with other well-known plasticity rules. A simplified phenomenological model is also derived, which should be useful for fast numerical simulation and analytical investigation of the impact of STDP at the network level.

1. Introduction

Spike-timing dependent plasticity (STDP) is a form of synaptic modification discovered relatively recently (Levy and Steward, 1983), which depends on the relative timing of pre- and post-synaptic spikes. Experiments *in vitro* in cortical slices from young animals, and in hippocampal organotypic cultures, have shown that the sign of the change of synaptic strength depends on the temporal order between pre- and post-synaptic spikes. More specifically, in cortical and hippocampal excitatory synapses, when the presynaptic event precedes the postsynaptic event by less than 50 ms, synaptic strength is reinforced, whereas the reverse temporal order leads to a depression of synaptic strength (Markram et al, 1997; Bi and Poo, 1998; Feldman, 2000). Reverse-sign STDP rules have also been found, in cerebellum-like structures (Bell et al. 1997). However, the presence of STDP *in vivo* and its applicability in the intact brain are still debated, which motivates building computational models.

Long-term potentiation (LTP) is a classical form of associative synaptic plasticity, which is known to be triggered by changes of intracellular calcium concentration (Lynch et al, 1983; Lisman, 1985, 1989; Malenka et al, 1988). Similarly, some forms of long-term depression (LTD) have been shown to be tightly linked to intracellular Ca^{2+} (Mulkey and Malenka, 1992; Brocher et al, 1992; Cummings et al, 1996). Based on the relative similarity of activity patterns leading to STDP with those leading to LTP and LTD, and on the reversibility of synaptic changes in a single pathway, it has been suggested that Ca^{2+} is the trigger for both components of STDP (Lisman, 1985, 1989; Bear et al., 1987; Artola and Singer 1993; Gold and Bear, 1994; Castellani et al., 2001; Shouval et al 2002, Karmarkar et al 2002). However, the biophysical mechanisms underlying STDP are still subject to controversy.

We present here a biophysical model of STDP which explores the calcium hypothesis. We show that this model can reproduce the phenomenology of STDP based on interactions between isolated pairs of pre- and post-synaptic spikes (STDP curve). In addition, the model is consistent with other – more complex – experimental paradigms involving higher-order interactions between spikes (spike-frequency dependence, spike triplets). Even though this biophysical model is quite simple compared to the actual enzymatic cascades underlying synaptic plasticity, it involves several differential equations

per synapse and would require huge computational resources if it had to be used in network simulations with several thousand synapses. To investigate networks, and in particular using more formal models such as the integrate-and-fire model, we need to simplify this biophysical model. Therefore, we also investigated simplified models of STDP, which are fast to simulate numerically and therefore more suitable for network simulations. We compare the performance of these two models in the case of spike triplet interactions.

2. Biophysical model of spike-timing dependent plasticity

2.1. *Experimental motivation of the model*

The biophysical model is based on recent measurements of calcium dynamics using fluorescent dyes. One of the main technical problems of such measurements is that the dye acts as a buffer for free calcium, so that the fluorescence signal does not reflect the real amplitude and kinetics of calcium transients. A recent method to take this bias into account revealed that intracellular calcium kinetics is much faster than previously thought (Sabatini et al, 2002): the calcium signal in a spine due to a backpropagating action potential (BAP, initiated in the soma) has a relatively fast decay time (around 15 ms), and reaches high values (up to 1 μM). In contrast, the calcium signal associated with an EPSP has a much longer decay time (around 80 ms), and a smaller amplitude (around 800 nM; see details in Sabatini et al, 2002). Other studies have found that a supralinear addition of the calcium signals from the BAP and the EPSP can occur, but only when the BAP arrives in a window of 0–20 ms after the EPSP (Magee and Johnston, 1997; Stuart and Hauser, 2001). This is explainable by the voltage-dependent properties of NMDA receptors, which increase the permeability to calcium only when the EPSP and the BAP coincide. The amplification of calcium signals due to opening of NMDA receptors can be a factor of around 3 to 4 in distal dendrites (300 μm from the soma; Magee and Johnston, 1997). We took into account the above experimental data in modelling calcium kinetics, as well as in setting the values of the NMDA conductance and the calcium channel density in dendrites and spines. We describe below how the biophysical model was constructed based on a simplified neuronal structure.

The second part of the model concerns the mechanism which translates calcium signals into plasticity. Theories relating calcium and plasticity are often related to the “BCM” theory of Bienenstock, Cooper, and Munro (Bienenstock et al, 1982). This model is based on experimental data on synaptic modification in the visual cortex during development: when the activity of the postsynaptic neuron (evoked by sensory input) is below a given threshold, the synapse is depressed (LTD), whereas if the evoked postsynaptic activity exceeds that threshold, the synapse is potentiated (LTP). The “ABS” model of Artola, Brocher and Singer (Artola et al., 1990) is directly deduced from the BCM theory and its generalization (Bienenstock et al., 1982; Bear et al., 1987). In the ABS model, the parameter used to characterize postsynaptic activity is the calcium signal in the postsynaptic spine rather than spike activity or postsynaptic membrane potential, and a second, lower postsynaptic threshold is added. If the maximum of the calcium signal is below this lower threshold, nothing happens. Between the two thresholds, LTD is induced and above the higher threshold, LTP is induced. In the present model of STDP, we follow the straightforward idea that the sign and the amount of plasticity are determined by the peak amplitude of the calcium transient. Indeed, it has been shown that calcium is the principal trigger for induction of LTP/LTD (Neveu and Zucker, 1996; Yasuda and Tsumoto, 1996; Yang et al, 1999; Zucker, 1999; Cormier et al, 2001). High levels of calcium would preferentially activate protein kinases whereas low levels would activate phosphatases (Lisman, 1985). The induction of LTP and LTD appears to depend on the relative activity of kinases and phosphatases (Miller and Kennedy, 1986; for a review see Colbran 2004). When both enzymes are present, predominant kinase activity leads to LTP and predominant activity of phosphatase leads to LTD (Lisman, 1989).

The first step towards modeling STDP attempted to link the BCM theory with the reversible storage of graded information by the kinase/phosphatase balance (Lisman, 1985, 1989; Bear, 1995). In a more recent study, a BCM-like model was proposed to model STDP based on the peak calcium level and two thresholds, for LTD and LTP respectively (Shouval et al., 2002; see also Castellani et al., 2001). In this case, however, the “STDP curve” (the amount of change in synaptic strength as a function of the time delay between pre- and post-synaptic spikes) will necessarily present two local minima

(ie, two depression zones flanking potentiation), since the peak calcium has to cross the depression threshold twice, on its rising phase and its return phase. The second LTD window is as large as the first LTD window. When taking into account stochastic fluctuations (Shouval and Kalantzis, 2005), the second LTD window is greatly reduced, suggesting that it could not be observable experimentally. However, with the exception of one study (Nishiyama et al, 2000), no experimental study has shown evidence for such a second LTD window.

Another modelling study (Karmarkar and Buonomano, 2002) concluded that it is not possible to obtain a realistic STDP curve with only one coincidence detector. According to this view, LTP would depend only on the calcium signal, whereas LTD would be triggered only if calcium and glutamate are present at the same time in the synaptic cleft. Indeed, they obtained an STDP curve very close to the experimental results, with one LTP window and only one LTD window as expected. But the question is what could be the molecule sensitive to glutamate. Karmarkar and Buonomano (2002) suggested that this coincidence detector could be the mGluR pathway. In agreement with this, it has been shown (Oliet et al, 1997) that two distinct forms of LTD coexist in CA1 pyramidal cells, one which is dependent on the activation of NMDA receptors (NMDA-LTD in Dudek and Bear, 1992), and the other one which is dependent on the activation of metabotropic glutamate receptors (mGluRs). However, several lines of evidence argue against the mGluR pathway. First, the rise of calcium mGluR-dependent LTD comes from the activation of T-type Ca^{2+} channels (Oliet et al, 1997), which is incompatible with the calcium rise following the activation of NMDA receptors in the Karmarkar and Buonomano (2002) model. Second, the mGluR-dependent LTD is not occluded by NMDAR-dependent long term potentiation (Oliet et al., 1997). Third, the mGluR pathway is slow and could hardly account for such precise timing as is involved in STDP.

Another possibility would be that synaptic receptors may differentially influence plasticity according to different states or subunit composition. Such a model was proposed for STDP, based on two functional states of NMDA receptors, one leading to LTP and the other one to LTD (Senn et al, 2001). This hypothesis is supported by experiments showing that different subunits of the NMDA receptor (NR2A or NR2B) are differentially expressed with age and sensory experience (Carmignoto and Vicini, 1992; Nase et al., 1999; Quinlan et al., 1999), and that the exact subunit composition of NMDA receptors could determine the sign of plasticity (LTP or LTD; see Liu et al., 2004; Massey et al., 2004), although they are slow. Such a hypothesis of multiple states of NMDA receptors also implies two coincidence detectors, and is therefore conceptually equivalent to the model of Karmarkar and Buonomano (2002). Another recent model (Rubin et al., 2005) shows that it is possible to derive the STDP curve from calcium, when not only levels but also time courses of calcium signals are taken into account. This model reproduces several experimental results, in particular their STDP curve do not have a second LTD window. But the model involves many kinetic parameters for the LTP and LTD pathway, and is difficult to tune.

Here, we build a simple model which involves two coincidence detectors. The first one is sensitive to calcium and the second one to glutamate. Our model involves the kinetics of two enzymes, one sensitive only to calcium, which triggers LTP (we call this enzyme *LTP enzyme*, to simplify) and the other one, activated when both calcium and glutamate are present, triggers LTD (we call it *LTD enzyme*). The kinetic schemes underlying the activation of these enzymes were deliberately kept simple compared to the actual complexity of the enzymatic cascades involved (see Discussion), but the model incorporates realistic calcium signals, and realistic amplification of calcium signals according to the respective timing of pre- and post-synaptic spikes.

2.2. Description of the biophysical model

All the simulations were performed with the NEURON simulation environment (Hines and Carnevale, 1997). We constructed a simplified neuron, consisting of a soma, a dendrite of length $L=1000\ \mu\text{m}$ (the typical apical dendrite length of deep-layer cortical pyramidal cells), and a spine located on the dendrite at $500\ \mu\text{m}$ from the soma. An axon was also included to obtain realistic backpropagation of spikes; the axon contained axon hillock, initial segment, nodes of Ranvier and segments with myelin (see Fig. 1). Active currents were inserted as follows: voltage-activated Na^+ , delayed-rectifier K^+ , and muscarinic K^+ (Km; slow, non inactivating) channels were inserted into the soma, the dendrite, the spine and the axon (except for Km which was not present in the axon). The values of these densities, as well as passive properties, are in accordance with the values given in Mainen and Sejnowski (1996). Hodgkin-Huxley sodium and delayed-

rectifier potassium channels were modeled as described previously (Mainen and Sejnowski, 1996). Calcium-dependent potassium (KCa) and high-voltage activated Ca^{2+} channels were inserted in the dendrite and the spine. see web-site <http://www.cnl.salk.edu/zach/patdemo.html> for the mechanisms. In the spine: Passive properties: $g_{pas}=8.3 \cdot 10^{-5} \text{S/cm}^2$; $C_m=1 \mu\text{F/cm}^2$. Active properties (in $\text{pS}/\mu\text{m}^2$): $g_{Na}=35$; $g_{Kv}=30$; $g_{Km}=0.1$; $g_{KCa}=3$; $g_{Ca}=0.8$

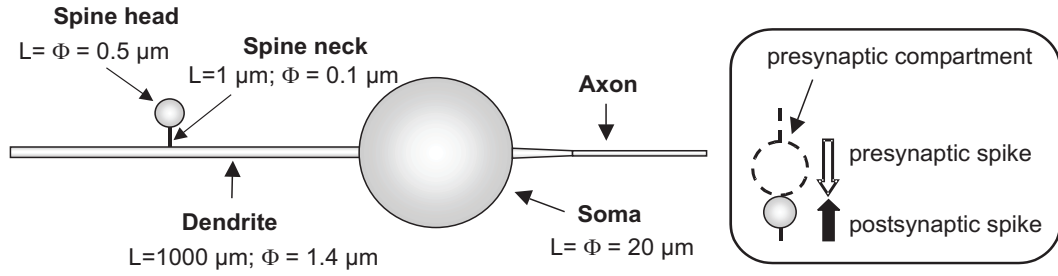


Fig. 1. Structure of the simplified neuron used in the simulations. The compartmental model comprises a soma, a dendrite, a spine and an axon (see text for details). STDP results from the temporal coincidence of a presynaptic action potential and a back propagating action potential in the spine (inset). Φ is the diameter, L the length of each compartment.

In these sections, an active calcium pump was also inserted (same model as in Destexhe et al, 1993). It has been shown that the main part of the calcium transient related to a BAP enters the cell through voltage-dependent calcium channels (Sabatini and Svoboda, 2000, Sabatini et al, 2002, Yuste and Denk, 1995) without a significant contribution from Ca^{2+} -induced Ca^{2+} -release (CICR). On the other hand, the calcium clearance is mediated both by smooth endoplasmic reticulum calcium ATPase pumps (SERCA pumps) and by plasma membrane Na^+ - Ca^{2+} exchangers or plasma membrane Ca^{2+} -ATPases (Holthoff et al, 2002; Markram et al 1995). These processes can be subsumed in one time constant decay τ_r (Holthoff et al, 2002). We took into account the endogenous buffering of the calcium by a numeric factor: it was estimated that the AP-evoked Ca^{2+} influx in the spine is of the order of $1 \mu\text{M}$, of which 5% stays free and the remainder binds to endogenous Ca^{2+} buffers (Svoboda et al., 2002) (factor 18 in the equation below).

Calcium pump: The calcium pump was described as a simple decay, with a time constant of $\tau_r=15 \text{ ms}$ (Sabatini et al 2002):

$$\frac{d[\text{Ca}]_i}{dt} = -\frac{I_{Ca}}{2Fd \times 18} + \frac{(Ca_\infty - [\text{Ca}]_i)}{\tau_r},$$

where $[\text{Ca}]_i$ is calcium concentration in the spine, I_{Ca} is the calcium current in the spine, F is the Faraday constant, $Ca_\infty=5 \times 10^{-7} \text{mM}$ is the calcium concentration in the spine at rest, and d is the depth of the submembranal shell to which this equation applies. The depth of the shell was set at $1/4$ of the diameter of the spine.

In some simulations, a mechanism for the diffusion of calcium from the dendrite into the spine was added (Holthoff et al, 2002). In this case, an additional term

$$-D([\text{Ca}]_i - [\text{Ca}]_d) \frac{S_{neck}}{L_{neck}V_{spine}}$$

was added in the equation above for the calcium pump. Ca_d is the calcium concentration in the dendrite, S_{neck} is the cross section of the neck ($S_{neck}=0.0078 \mu\text{m}^2$) and V_{spine} is the volume of the spine ($V_{spine}=0.065 \mu\text{m}^3$). These values correspond to morphological measurements (Harris and Kater, 1994).

Kinetic models for AMPA and NMDA receptors were inserted in the spine, based on the model of Destexhe et al. (1994, 1998; see web-site <http://www.iaf-cnrs-gif.fr>).

AMPA receptors:

The AMPA-mediated conductance is modeled according to Destexhe et al. (1994): AMPA receptors are represented by a two-state (open-closed) kinetic scheme, and when a presynaptic potential occurs, a short pulse (1 ms, 1 mM) of glutamate is delivered to the receptors. This is equivalent to model the AMPA conductance by the following equations:

$$\frac{dm}{dt} = \alpha T (1 - m) - \beta m ,$$

where m represents the fraction of receptors in the open state, α and β are the forward and backward rate constants, and T is the concentration of glutamate in the synaptic cleft. The conductance is given by $g_{AMPA} = \bar{g}_{AMPA} m$ where $\bar{g}_{AMPA}=0.5$ nS is the maximal conductance of the synapse. The rate constants were estimated from fitting this model to whole-cell recordings of AMPA-mediated currents in hippocampal pyramidal cells (Destexhe et al., 1998).

NMDA receptors:

A two-state kinetic model was used to model NMDA receptors according to a similar scheme as above (see Destexhe et al., 1998, for kinetic parameters and their estimation from experimental data). This model was modified to calculate the calcium current. We used the GHK equation for the calcium current (Goldman, 1943; Hodgkin and Katz, 1949):

$$I_{Ca} = P_{Ca} B(V) m G(V, [Ca]_o, [Ca]_i) ,$$

where $P_{Ca}=4.6925(\text{cm}^3 \text{ mV/Cb})$ is the permeability to calcium, m is the fraction of open receptors. The permeability was adjusted such that 10% of the current is Ca^{2+} -mediated at -40mV. $B(V)$ represents the voltage dependence of NMDA currents (Jahr and Stevens, 1993):

$$B(V) = \frac{1}{1 + \exp(-0.062 V) [Mg]_o/3.57} ,$$

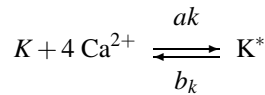
where $[Mg]_o=1$ mM is the external magnesium concentration. $G(V, [Ca]_o, [Ca]_i)$ is a nonlinear function of voltage and ionic concentrations:

$$G(V, [Ca]_o, [Ca]_i) = Z^2 F^2 V / RT \frac{[Ca]_i - [Ca]_o \exp(-ZFV/RT)}{1 - \exp(-ZFV/RT)}$$

where $Z=2$ is the valence of calcium ions, F is the Faraday constant, R is the gas constant and T is the temperature in Kelvin. $[Ca]_i$ and $[Ca]_o=1.5$ mM are the intracellular and extracellular Ca^{2+} concentrations (in M), respectively. \bar{g}_{NMDA} was set to 0.3 nS to have realistic NMDA currents compared to AMPA currents. This gives a ratio of NMDA/AMPA EPSC of about 0.5, as observed experimentally (Feldmeyer et al, 2002) and calcium signals similar to experiments (Sabatini et al., 2002). EPSPs in the spine were triggered by action potentials in the presynaptic compartment. Backpropagating action potentials were initiated by a brief current pulse in the initial segment.

In addition to postsynaptic receptors, the postsynaptic compartment in the spine contained mechanisms for regulating synaptic strength using LTP and LTD enzymes, obeying the following kinetic schemes:

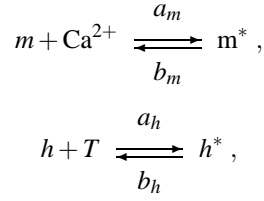
LTP enzyme:



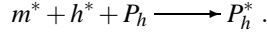
where K^* and K represent respectively the activated and non-activated forms of the LTP enzyme, with corresponding rate constants a_k and b_k .

It is known that the first step of the long pathway of auto-phosphorylation of Ca^{2+} /calmodulin-dependent protein kinase (CaMKII) begins with the formation of the complex Ca^{2+} /calmodulin which involves 4 Ca^{2+} ions per molecule of calmodulin. Here, we simplified the cascade of reactions happening in this process of auto-phosphorylation (Hanson and Schulman, 1992), but we kept the selectivity for calcium: our LTP enzyme will be activated only for high peak calcium signals.

LTD enzyme:



and



Here, T represents the transmitter (glutamate) during a synaptic release event, m and h are enzymes such that one is activated by calcium, the other is activated by glutamate, and both need to be present in activated form (m^* and h^*) to activate the LTD enzyme P_h . a_m, b_m, a_h, b_h are rate constants.

The rate constants parameters were $a_k = 3 \cdot 10^9 \text{ mM}^{-4} \text{ ms}^{-1}$; $b_k = 1 \text{ ms}^{-1}$; $a_m = 200 \text{ mM}^{-1} \text{ ms}^{-1}$; $b_m = 0.1 \text{ ms}^{-1}$; $a_h = 1 \text{ mM}^{-1} \text{ ms}^{-1}$; $b_h = 0.4 \text{ ms}^{-1}$. $K = b_k/a_k$ has been chosen such as the LTP enzyme is triggered when the amount of calcium is higher than $3.5 \mu\text{M}$ (the concentration of K^* as a function of calcium is a sharp sigmoid with an inflexion point at $3.5 \mu\text{M}$ calcium). The rate parameters for the LTD enzyme have been chosen such as there is no plasticity for large $t_{\text{post}} - t_{\text{pre}}$ (positive or negative), and the maximum amount of LTP should be almost twice the maximum amount of LTD (Bi and Poo, 1998). When a_m or a_h are reduced, the LTD window becomes smaller and the maximum LTD is reduced.

The amount of LTP (LTD) is directly proportional to the maximum value of the concentration of K^* (P_h^*) with a factor 1.67: in this case, a concentration of 0.6 of the enzyme lead to 100% potentiation (depression). For simplicity, we omitted possible additional enzymes which would no be degraded and would keep the peak concentration. The total plasticity is computed as the difference between LTP and LTD contributions (cf. Figs. 2 and 3). No saturation of potentiation or depression was introduced, therefore the amount of plasticity is the same after each pairing. This enables us to use only one pairing to compute STDP curves or triplet maps (see below).

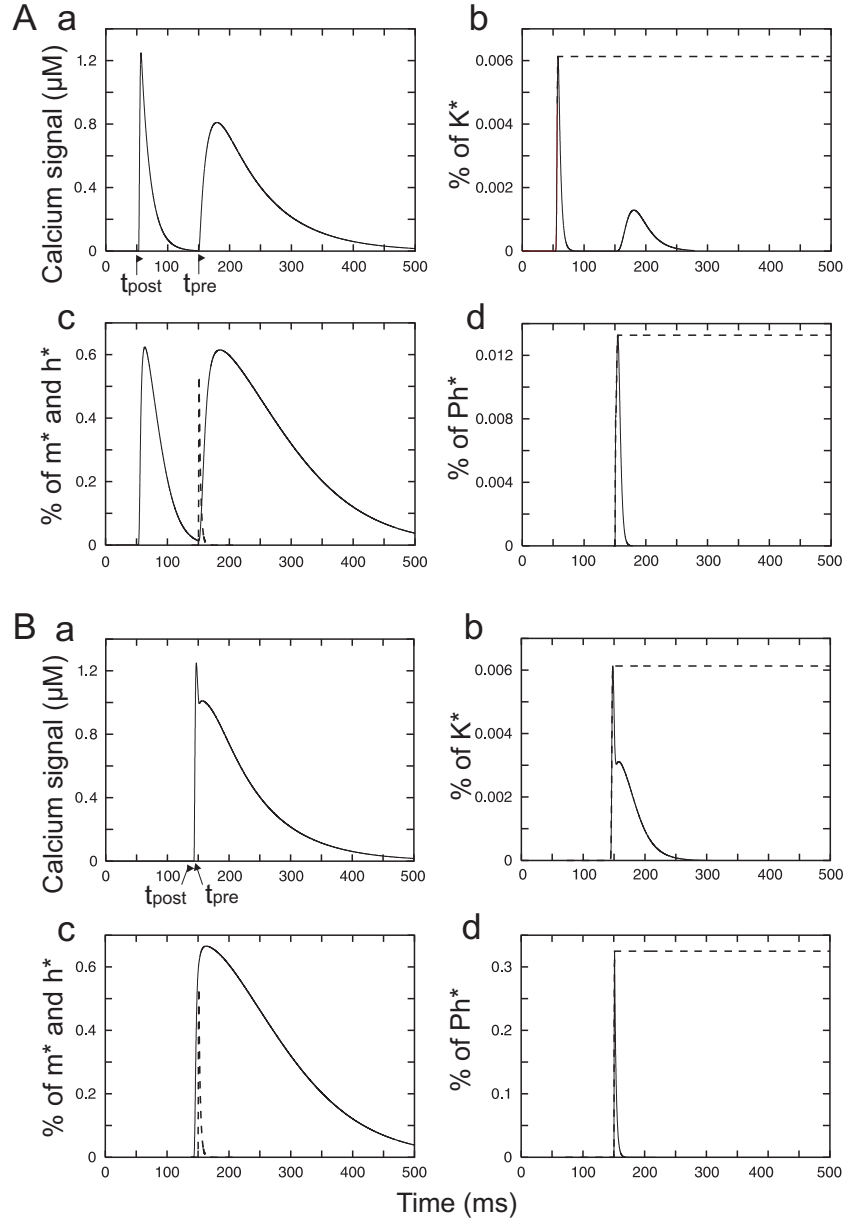


Fig. 2. Response of the model when the postsynaptic spike occurs prior to the presynaptic spike, in terms of calcium signals and enzyme concentrations, and showing the measures of plasticity in the model. A. The difference of timing between pre- and post-synaptic spikes is $t_{\text{post}} - t_{\text{pre}} = -100$ ms. B. $t_{\text{post}} - t_{\text{pre}} = -10$ ms. a: calcium concentration in the spine; b: fraction of activated LTP enzyme (the dashed line shows the maximum of this function; LTP is directly proportional to this value); c: fraction of activated m -enzyme (continuous line) and of h -enzyme (dashed line; see details in text); d: fraction of activated LTD enzyme (the dashed line is the maximum of this function; LTD is directly proportional to this value). $a_k = 3 \cdot 10^9 \text{ mM}^{-4} \text{ ms}^{-1}$; $b_k = 1 \text{ ms}^{-1}$; $a_m = 200 \text{ mM}^{-1} \text{ ms}^{-1}$; $b_m = 0.1 \text{ ms}^{-1}$; $a_h = 1 \text{ mM}^{-1} \text{ ms}^{-1}$; $b_h = 0.4 \text{ ms}^{-1}$.

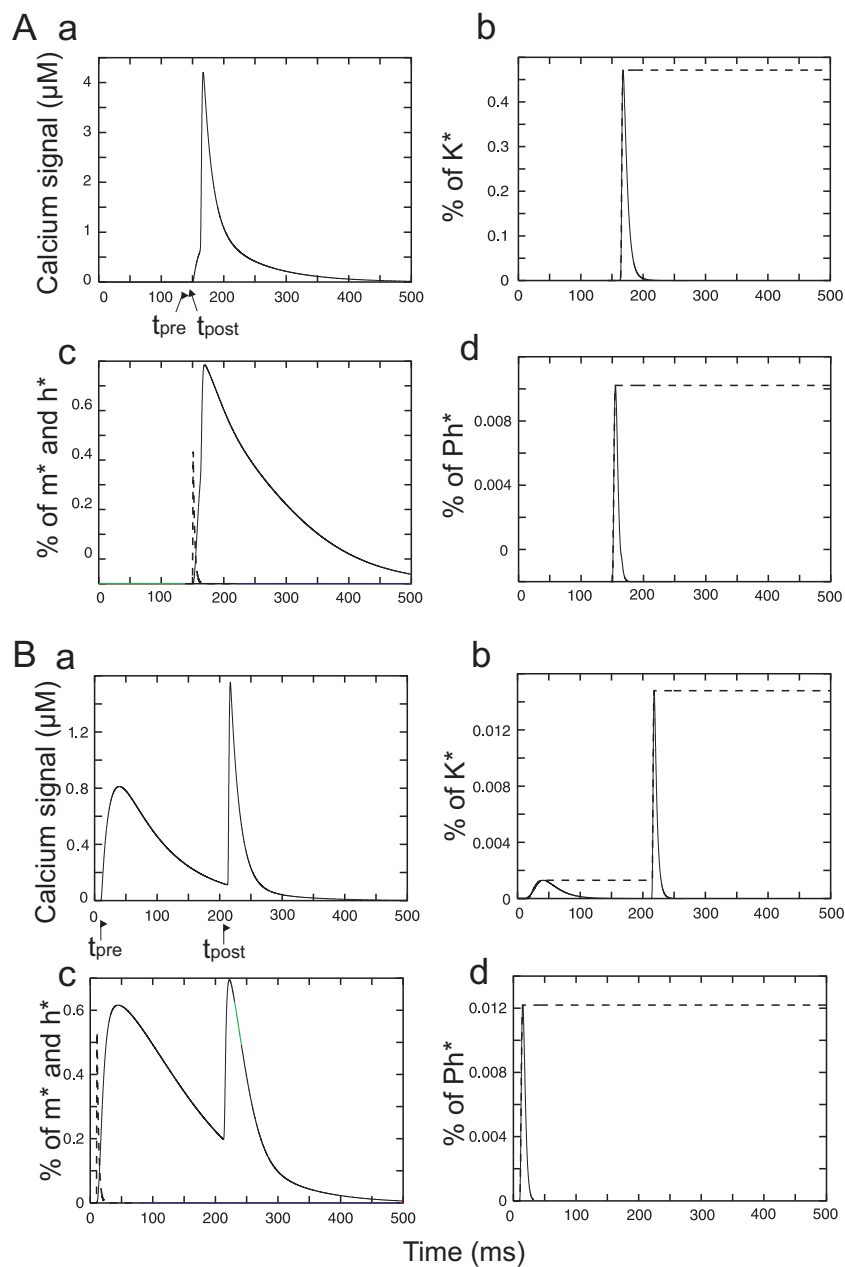


Fig. 3. Response of the model when the postsynaptic spike occurs after the presynaptic spike. Description similar to that of Fig. 2 (note change of scale for some of the curves). A. $t_{\text{post}} - t_{\text{pre}} = +10$ ms. B. $t_{\text{post}} - t_{\text{pre}} = +200$ ms.

3. Simplified phenomenological model of spike-timing dependent plasticity

The biophysical model contains several differential equations for each synapse, and would require huge computational resources if it had to be used in network simulations involving several thousands of synapses. To investigate networks, and in particular networks using more formal models such as the integrate-and-fire model, we need to simplify this biophysical model.

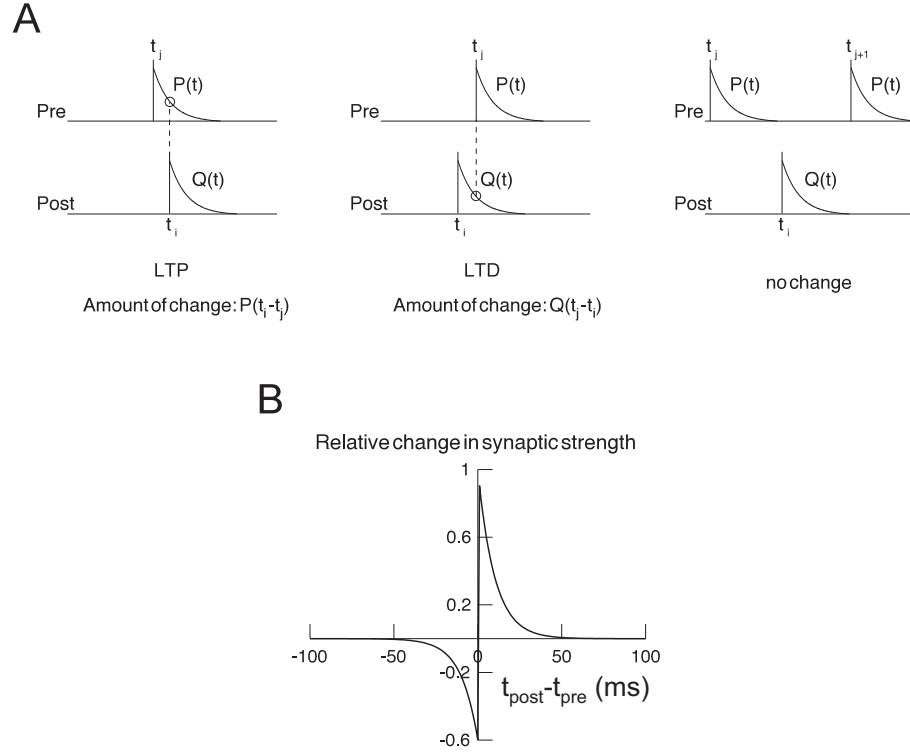


Fig. 4. Phenomenological model of STDP. A. Schematic description of the model. The use of exponential functions $P(t)$ and $Q(t)$ allows us to have a general rule to capture the phenomenology of long-term potentiation (LTP), long-term depression (LTD) or no change, as a function of the respective timing of pre- (t_j) and post-synaptic spikes (t_i). The exponential functions can be adjusted in order to match experimental data. B. Simulation of the model for pairs of pre- and post-synaptic spikes with different relative timing. The relative change in synaptic strength is indicated as a function of the time difference between pre- and post-synaptic spikes (spike timing).

The first type of simplification is to remove the differential equations describing the kinetics of calcium, enzymes and ion channels, and replace these dynamic variables by a functional dependence of the plasticity on the timing of pre- and post-synaptic spikes. Noting that the enzymes that trigger LTP and LTD both follow exponentially-decaying time courses, we can replace these signals by ad-hoc exponential functions. This leads to a model in which the amount and sign of plasticity are given by two of such exponential functions, which we call P and Q , and which are triggered by pre- and post-synaptic spikes, respectively (Fig. 4A). The amount of the plasticity change is then given by the value of these exponential functions at the time of the post- and pre-synaptic spike, respectively (Fig. 4A, circles). This scheme is one of the simplest possible ways to convert the timing of pre- and post-synaptic spikes into the amount of STDP. This model can be put in equation form, in which the time derivative of the synaptic weights is given by:

$$\frac{d\omega_{ji}}{dt} = \sum_k P[t - \tilde{t}_j(t)] \delta(t - t_{i,k}) - \sum_l Q[t - \tilde{t}_i(t)] \delta(t - t_{j,l}), \quad (1)$$

where ω_{ji} is the synaptic strength of the synapse from neuron j (presynaptic) to neuron i (postsynaptic). The sum runs

over all postsynaptic and presynaptic spike times ($t_{i,k}$ and $t_{j,l}$, respectively; the function $\tilde{t}_i(t)$ gives the time of the last spike that occurred in neuron i at time t). P and Q are respectively the functions describing the amount of LTP and of LTD as a function of the timing of spikes. This model assumes that LTP occurs at the time of the postsynaptic spike (term $\delta(t - t_{i,k})$) if a presynaptic spike occurred in a short, preceding time window (which is encoded by the function P) and that LTD occurs at the time of the presynaptic spike, if a postsynaptic spike has occurred previously (encoded by the function Q). This model can be simplified by only summing over the spikes immediately preceding in time. The exponential functions P and Q are given by:

$$P(t) = \exp[-t/\tau_p] \quad , \quad Q(t) = \exp[-t/\tau_q]$$

where τ_p and τ_q are adjustable time constants which can be obtained either from the biophysical model, or by directly fitting them to experimental data (see below). In this form, these equations are very similar to previously proposed phenomenological models of STDP (Song et al., 2000).

Two additional mechanisms can be incorporated in this model at minimal computational expense. The first addition is the inclusion of triplet interactions. Experiments showed that the nonlinear interaction between successive pairs of pre- and post-synaptic spikes can be captured by a suppression factor which modulates the amount of synaptic change according to previous history (Froemke and Dan, 2002):

$$\epsilon_i = 1 - \exp[-(t_i - t_{i-1})/\tau_s]$$

where t_i and t_{i-1} are two successive spikes of neuron i , and τ_s is the suppression time constant. This factor ϵ_i is specific to every spike, and can be different whether the spike is presynaptic or postsynaptic. The magnitude of synaptic plasticity is then given by

$$\frac{d\omega_{ji}}{dt} = \epsilon_j \epsilon_i \left[\sum_k P[t - \tilde{t}_j(t)] \delta(t - t_{i,k}) - \sum_l Q[t - \tilde{t}_i(t)] \delta(t - t_{j,l}) \right]. \quad (2)$$

The use of suppression factors $\epsilon_{i,j}$ introduces a form of refractoriness to synaptic change, and experimental measurements have shown that the interaction between triplets is optimally fit using suppression time constants of 28 ms for presynaptic spikes and 88 ms for postsynaptic spikes (Froemke and Dan, 2002).

The second addition was to incorporate saturating mechanisms (see for example Levy and Desmond, 1985). In the above model, synapses are non-saturable, which means that the values of ω_{ji} can increase to arbitrarily large values, or decrease to arbitrarily low values and even become negative, which has no physical sense. To solve this problem, we need to consider a more complex equation with saturating terms

$$\frac{d\omega_{ji}}{dt} = \epsilon_j \epsilon_i \left[(\omega_{ji} - \omega_{LTP}) \sum_k P[t - \tilde{t}_j(t)] \delta(t - t_{i,k}) + (\omega_{ji} - \omega_{LTD}) \sum_l Q[t - \tilde{t}_i(t)] \delta(t - t_{j,l}) \right], \quad (3)$$

where ω_{LTP} and ω_{LTD} are the saturating values of synaptic strength for LTP and LTD, respectively, which obey the relation: $\omega_{LTD} < \omega_{ji} < \omega_{LTP}$.

This model is still computationally efficient, because we stay within a framework in which changes are to be made only when a spike occurs (in either the pre- or the post-synaptic cell). The rest of the time (when no spike occurs), no calculation need be performed. Indeed, there was no detectable difference of computational performance between the model with and without saturating terms (Eqs. 2 and 3, respectively). There was, however, a difference concerning the asymptotic convergence of synaptic weights. STDP rules with artificial saturation (“hard” bounds) lead to a bimodal distribution of synaptic weights (Song et al., 2000). By contrast, the presence of saturation (“soft” bounds) leads to convergence of synaptic weights towards an attractor value in between the boundaries (van Rossum et al., 2000; Gutig et al., 2003). The

latter behavior was also present in this model (Fig. 5).

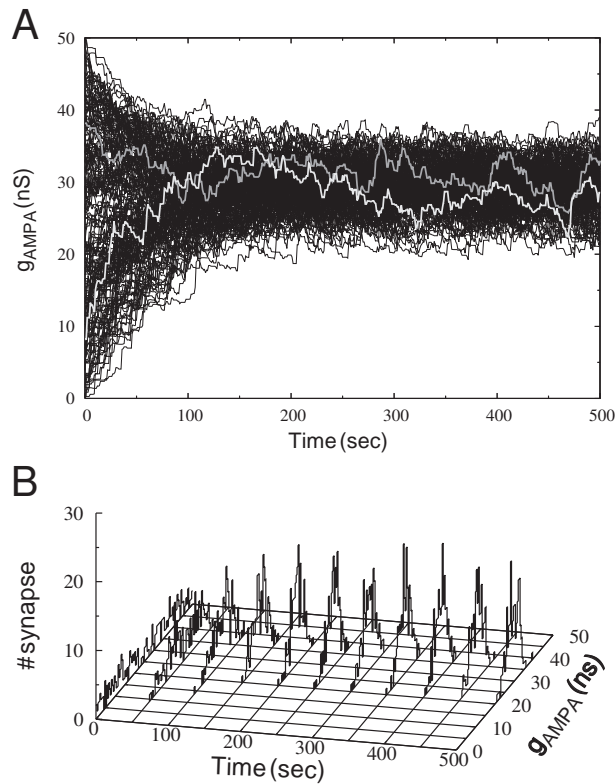


Fig. 5. Asymptotic convergence of synaptic weights in the phenomenological model of STDP. A single-compartment spiking neuron received 200 excitatory synapses subject to STDP as described by the phenomenological model (Eq. 3). Every synapse released randomly according to a Poisson process (mean rate of 1 Hz), which drove the postsynaptic neuron to fire occasionally (average rate of 9.2 Hz), leading to LTP or LTD at excitatory synapses. A. Convergence of synaptic weights during a 500 s simulation. Two of the weights are highlighted using a different color (gray and white) to illustrate individual excursions. B. Distribution of synaptic weights calculated every 50 s. The weights converge towards a single-peaked (unimodal) distribution after roughly 200 s.

4. Results

4.1. STDP curve and dependence to frequency

We now confront the models with experimental procedures usually used to produce either LTP or LTD, either in simple cases of STDP, or in more complex cases such as low and high frequency stimulation, or complex spike patterns. The simplest form of STDP curve is based on measurements of plasticity following isolated pairs of pre- and post-synaptic spikes of variable time intervals (Bi and Poo, 1998). This type of STDP curve can be reproduced by the model, and it

presents only two windows, one of LTP and one of LTD, as expected (Fig. 6).

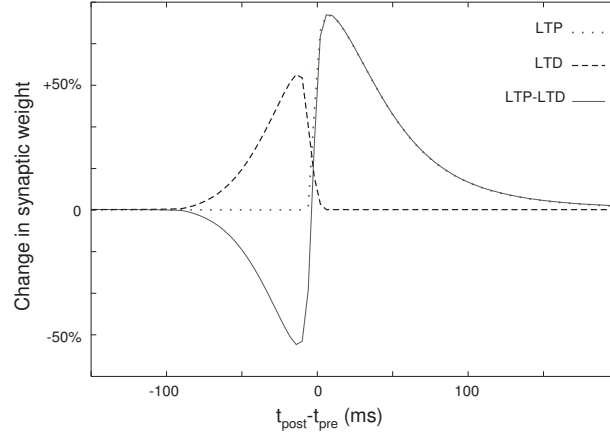


Fig. 6. STDP curve in the biophysical model. The dashed curve represents LTD and the dotted curve represents LTP. The total change in synaptic weight is computed as LTP-LTD (continuous line).

The STDP curve can also be simulated using the simplified model, by calculating the output of Eq. 3 for different timings between pre- and post-synaptic spikes (Fig. 4B). The relative changes of synaptic weight were chosen to match the STDP curve measured experimentally on cultured hippocampal neurons (Bi and Poo, 1998).

We next confronted the biophysical model with more biologically realistic situations: the dependence of the STDP curve on pairing frequency. The qualitative behavior of the model (Fig. 7A) is very close to the experimental results: beyond a certain frequency, only LTP is present even for negative time intervals, which give LTD for smaller frequency (Sjostrom et al., 2001). Our threshold frequency is around 15 Hz, which is lower than the threshold of around 40–50 Hz reported experimentally. This effect was not predicted by the simplified model (Fig. 7B).

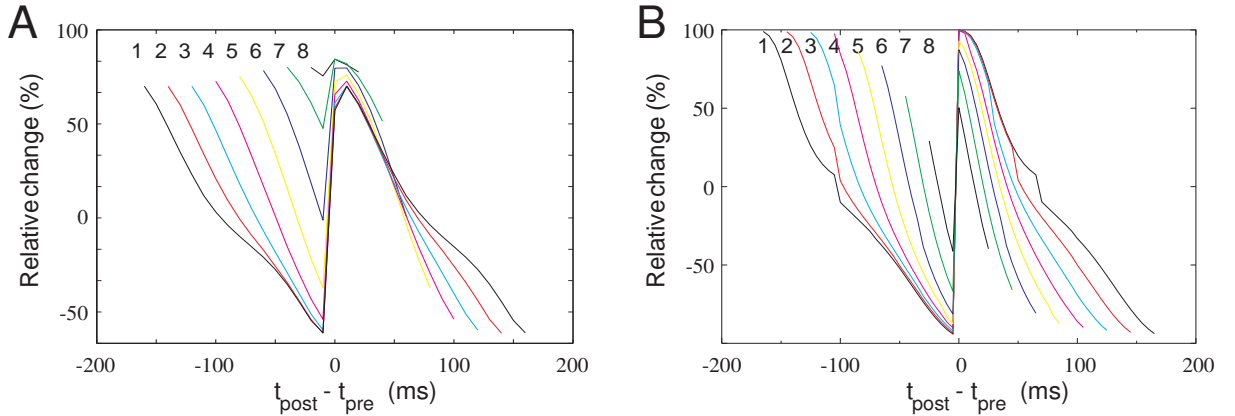


Fig. 7. STDP curve as a function of the frequency of the pairings. 5 pairings were done for each frequency and each time intervals. A. Biophysical model. B. Simplified model (see text for description). In both cases, the period was varied from 170 ms (frequency of 5.9 Hz) to 30 ms (frequency of 33.3 Hz), in steps of 20 ms (curves labeled from 1 to 8). Only the biophysical model qualitatively reproduces the experimental findings of Sjostrom et al. (2001).

Another constraint for models is that, in the absence of postsynaptic spikes, repeated presynaptic activity should lead to potentiation and depression at high or low frequency respectively (Dudek and Bear, 1992, Kirkwood and Bear, 1994). This behavior was also present in the biophysical model (Fig. 8): for small frequencies (smaller than 2.5 Hz; equivalent to

time intervals larger than 400 ms), there is no plasticity because the calcium signal stays subthreshold for triggering LTP or LTD. For larger frequencies (between 2.5 and 35 Hz), the calcium concentration reaches moderate levels, and LTD is observed. For high frequencies (> 35 Hz), the calcium signal reaches its highest level, and LTP is observed.

Our transition frequency between LTD and LTP is 35 Hz, whereas experimentally, the transition frequency is around 10 Hz. This discrepancy can be explained because there is no postsynaptic spikes in the model, whereas in experiments, high-frequency LTP is likely to elicit postsynaptic spikes. Another parameter could influence the transition frequency: the transition frequency between LTD and LTP decreases as the AMPA conductance increases (data not shown). Even if we set the AMPA and NMDA conductances in our model to have realistic currents (cf above), we could increase the AMPA conductance to have a smaller transition frequency.

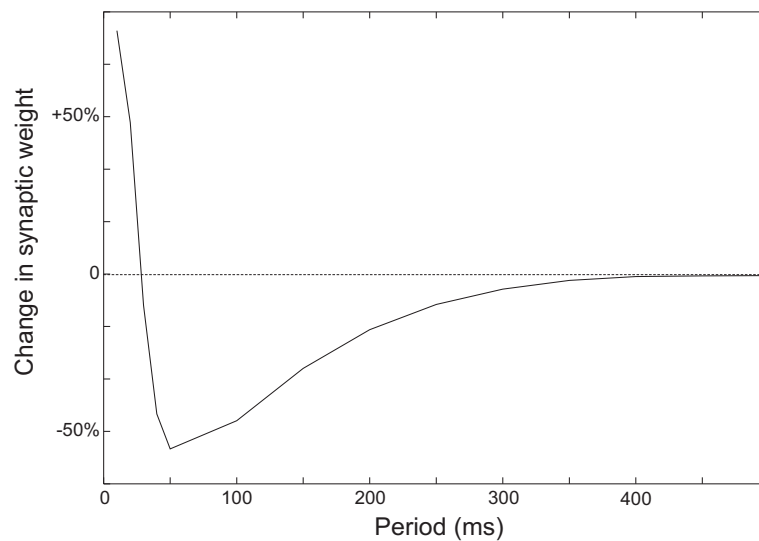


Fig. 8. Plasticity as a function of the time interval between presynaptic events (in this case, there is no postsynaptic spike). The model qualitatively reproduces experimental results (Dudek and Bear, 1992; Kirkwood and Bear, 1994).

In Fig. 6, although the general shape of the curve is correct, one can object that the LTP window is too large, and the LTD window too narrow: LTP is typically observed experimentally when the delay Δt between pre- and post-synaptic spikes is in the range $0 < \Delta t < 50$ ms, whereas LTD is observed for $-100 \text{ ms} < \Delta t < 0$ (Bi and Poo, 1998). To test for possible sources of this discrepancy, we varied the kinetics of NMDA channels: when their decay was faster, the LTP window was narrower (not shown), which may explain this effect. Another possible explanation is related to calcium diffusion: calcium can diffuse from the dendrite into the spine (Holthoff et al., 2002) and this diffusion is inversely proportional to the length of the spine neck. Some studies (Sabatini et al., 2002) have shown that the BAP calcium signal in the spine can be described by a single exponential, because calcium in the dendrite and spine have similar decay kinetics (20 ms in dendrite, 15 ms in spine). In some cases, however, these kinetics can be very different. In spines attached to thicker dendrites for example, the decay of the calcium transients due to a BAP must be fitted by two exponentials, the fastest time constant reflecting the time decay of the calcium in the spine whereas the slow time constant reflects the slower decay of calcium in the dendrite. To study the influence of calcium diffusion, we set the time constant of the pump in the dendrite to be much larger than in the spine, around 70 ms (Holthoff et al., 2002). When diffusion is present, the calcium transient presents a long-lasting tail (Fig. 9), which enlarges the LTD window in the STDP curve (Fig. 10). This effect was seen in experiments (Holthoff et al., 2002): proximal spines, which on average experience slower calcium decay kinetics, undergo more depression in comparison to distal spines, which can clear calcium faster. This is also consistent with artificially slowed calcium decay kinetics in spines and dendrites by applying cyclopiazonic acid (CPA), a SERCA pump inhibitor (Holthoff et al., 2002). When we incorporated the effect of diffusion and a shorter decay time constant for the NMDA

synapse, the model displayed an STDP curve much closer to experiments (Fig. 10) (Bi and Poo, 1998; Froemke and Dan, 2002).

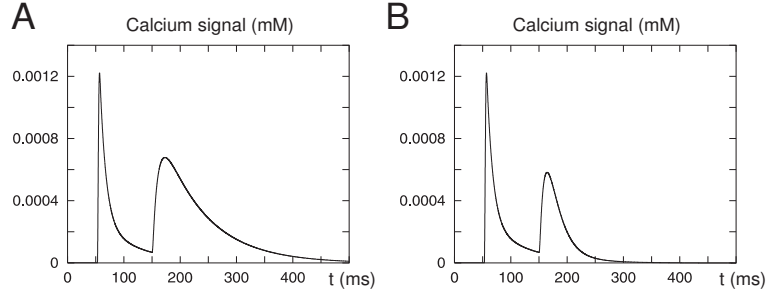


Fig. 9. Calcium concentration in the spine when diffusion of free calcium from the dendrite into the spine is taken into account. The diffusion coefficient of the free Ca^{2+} is $D = 0.22 \mu\text{m}^2/\text{ms}$ (Allbritton et al, 1992). A. Time decay of NMDA receptors is 80 ms; B. Time decay of NMDA receptors is 20 ms.

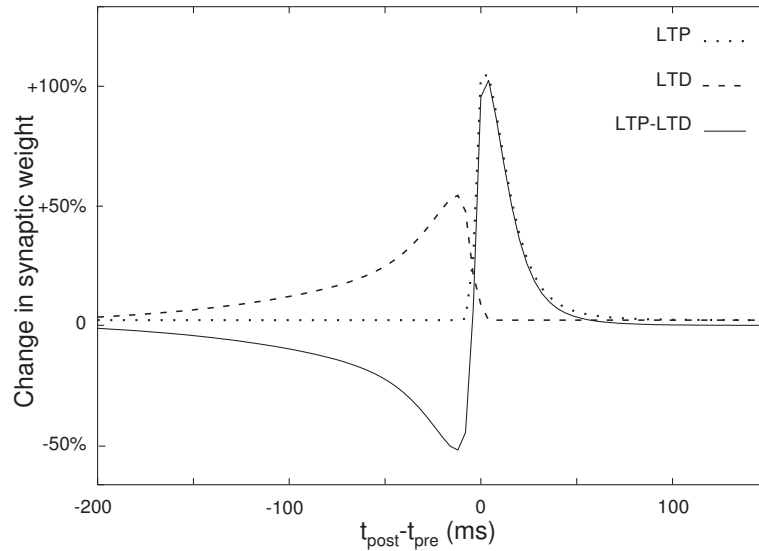


Fig. 10. STDP curve in the model incorporating calcium diffusion. The time constant for NMDA decay is of 20 ms. $a_k = 3 \cdot 10^9 \text{ mM}^{-4} \text{ ms}^{-1}$; $b_k = 0.25 \text{ ms}^{-1}$; $a_m = 200 \text{ mM}^{-1} \text{ ms}^{-1}$; $b_m = 0.1 \text{ ms}^{-1}$; $a_h = 1 \text{ mM}^{-1} \text{ ms}^{-1}$; $b_h = 0.4 \text{ ms}^{-1}$. The LTP window is shorter than the LTD window, and is around 50 ms. The LTD window is around 150 ms.

4.2. Spike triplets

We next studied the interactions between multiple pre- or post-synaptic events. Besides previous indirect evidence (Bi and Poo, 1998; Boettiger and Doupe, 2001), a single study (Froemke and Dan, 2002) investigated specifically the role of spike triplet interactions in the framework of STDP. These experiments considered multiple-pairing paradigms consisting of spike triplets, with two possible pre-post associations, characterized by two time delays, as shown in Fig. 11A. The main finding was that the plasticity observed is not a linear summation of the plasticity predicted by the STDP curve applied separately to the two pairs of spikes, but that there was a nonlinear interaction in which the effect of the first pair tends to prime over that of the second one (Froemke and Dan, 2002). The plasticity observed is represented in Fig. 11B (left panels)

and is well predicted by an interpolation function based on an exponential suppression factor ϵ (Fig. 11B, right panels).

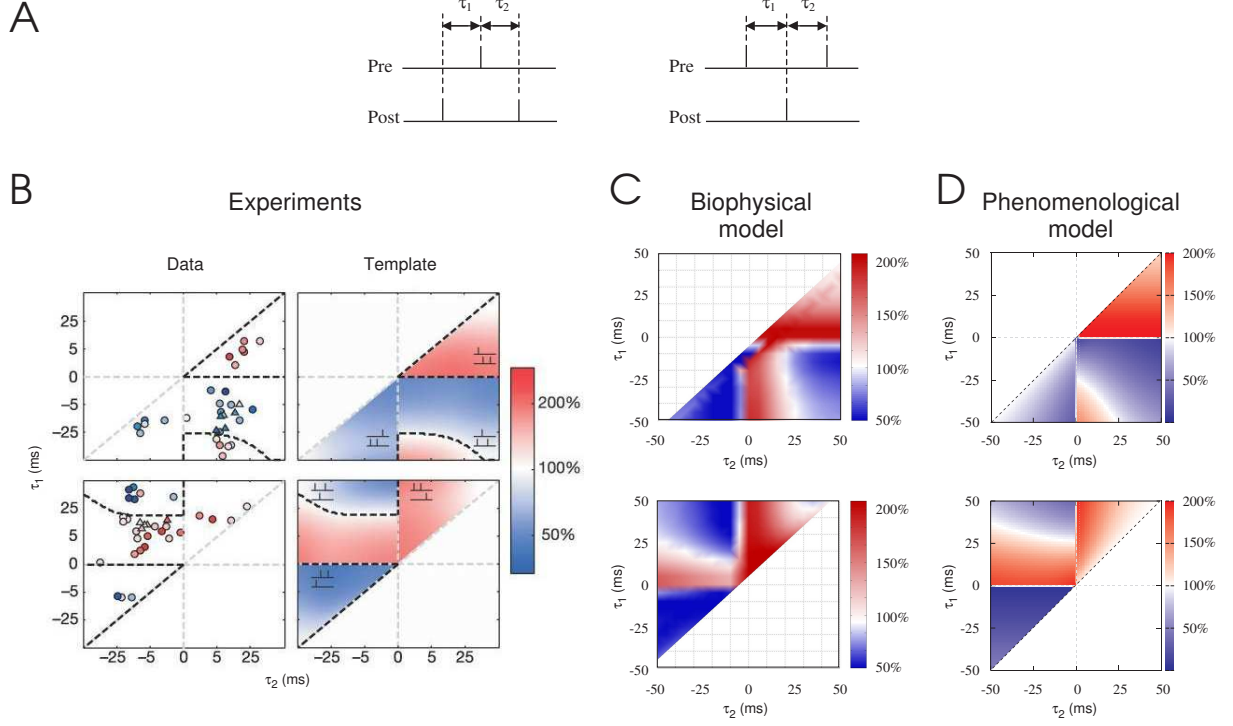


Fig. 11. Spike-timing dependent plasticity for spike triplets. A. Scheme of interaction between “1pre-2post” triplets (left: one presynaptic event paired with two postsynaptic events), and “2pre-1post” triplets (right: two presynaptic events paired with one postsynaptic event). τ_i ($i=1,2$) is defined as in Froemke & Dan (2002), $\tau_i = t_{post} - t_{pre}$. B. Experimental data from Froemke & Dan (2002). Different pairings were realized at different latencies according to the scheme in A (top graphs refer to 1pre-2post triplets, while 2pre-1post triplets are shown in bottom graphs; shades of red indicate potentiation, blue depression – see scale). The left panels show a template function model that extrapolates the experimental data. C. Simulation of the same pairing protocols using the biophysical model. Diffusion was present and the time constant for NMDA decay was 20 ms. D. Simulation of the same protocol using the phenomenological model (see text for details).

The same paradigm was simulated using the biophysical model (Fig. 11C). The qualitative agreement with experiments is remarkable, although there is no need to introduce any type of spike efficacy or suppression factor in this model. In the triplet map, the maximum potentiation is 100% and the maximum depression is 50% of the initial synapse strength: these values corresponds to those observed in Froemke and Dan (2002) experiments, in their STDP curve and in their triplet map. However, some details differ: in Froemke and Dan’s scheme, the two diagrams 1pre-2post and 2pre-1post can be deduced one from the other by a central symmetry and by replacing LTP by LTD and LTD by LTP. This is not the case in the biophysical model (compare color maps in Fig. 11B and C). For example, the LTP window in the parametric zone $\{ \tau_1 < 0, \tau_2 > 0 \}$ in the top diagram has not the same dimension as the LTD window in the parametric zone $\{ \tau_1 > 0, \tau_2 < 0 \}$ in the bottom diagram. Another difference is that saturation is not included in the biophysical model. Besides these differences with Froemke-Dan’s interpolation scheme, the agreement between the biophysical model and the experiments is excellent.

Finally, the same triplet paradigms were simulated using the simplified model (Fig. 11D). This model performs well in terms of capturing the nonlinear interactions between successive spike pairs (compare Fig. 11B and D). However, this well-behaved performance is “built-in” through the inclusion of the spike efficacy factors (ϵ in Eq. 3). Nevertheless, this model is orders of magnitude faster to simulate compared to the biophysical model, and should be useful for including STDP in large-scale network simulations.

5. Discussion

We have presented here two classes of models of STDP, and compared the behaviour of these models. The main result is that the biophysical model can reproduce many of the complex dependencies observed experimentally (frequency interactions; triplet interactions), without invoking additional “built-in” mechanisms. The same phenomenology was also present in a simplified model, but in this case the model had to incorporate specific “built-in” additional nonlinear mechanisms (such as the spike efficacy ϵ). We discuss here the advantages and pitfalls of these models with respect to the experimental data so far available, and delineate some possible applications.

The biophysical model is relatively simple in its structure. It is based on elementary kinetic schemes which represent a huge simplification of the actual complexity of the cascade of kinases and phosphatases from the calcium signal to its translation in terms of negative or positive plasticity. For example, the interactions involved in the activation of CaMKII are quite complex and more detailed models have been proposed based on these interactions (Zhabotinsky, 2000; D’Alcantara et al, 2003). Compared to another simplified biophysical model (Rubin et al., 2005) our model does not take into account only calcium levels, but also calcium kinetics. The difference is that our LTD enzyme depends on glutamate. Our model involves much less parameters, and should be easier to tune. It may also be less dependent of the exact shape of calcium signals. Although simple compared to the actual complexity of the synaptic machinery, the present biophysical model reproduces an STDP curve with the correct shape, and the width of the LTP and LTD windows can be varied by, respectively, taking into account the diffusion of the free calcium from the dendrite into the spine and changing the kinetics of the NMDA receptors. We found that calcium diffusion has to be taken into account and that the time decay of the NMDA-mediated calcium current should be around 20 ms, much shorter than the estimates from experiments (e.g., Sabatini et al., 2002). These predictions will need to be investigated further by appropriate experiments.

Another point which will require experimental verification is the prediction that LTD is due to an enzyme which is sensitive to glutamate. This component was essential for the model to account for experiments where the frequency of the pairing or of the presynaptic event (without postsynaptic events) is varied, as well as experiments on spike triplets. The possibility that this pathway could be mediated by the metabotropic glutamate receptor, acting as the second coincidence detector (Karmarkar and Buonomano, 2002), should be explored using more appropriate models.

A remarkable property of the biophysical model is that several properties, measured experimentally, emerge without requiring the incorporation of specific “built-in” nonlinear interaction mechanisms. These emergent properties are the frequency interactions (Fig. 7A), as described experimentally by Sjostrom et al. (2001), and the spike triplet interactions (Fig. 11C), as described experimentally by Froemke and Dan (2002). The mechanism underlying the latter interaction is illustrated in Fig. 12: the existence of LTP in the parametric zone $\{0 < \tau_1 < 25 \text{ ms}, \tau_2 < 0\}$ for the 2pre-1post interaction is explainable by nonlinear mechanisms. The amplification due to the short-time interaction pre-post is so strong that LTP is larger than LTD and the global plasticity LTP–LTD is positive, leading overall to LTP (Fig. 12) This type of interaction also constitutes a prediction of the model, which could be corroborated by appropriate experiments.

An apparent inconsistency of the biophysical model with Froemke and Dan’s experiments can be seen in the symmetric region for the 1pre-2post interaction ($\tau_1 < 0, 0 < \tau_2 < 25 \text{ ms}$): the biophysical model does not give LTD, as predicted by Froemke and Dan’s spike efficacy scheme. However, one could notice that Froemke and Dan have very few experimental data for $\tau_2 < 5 \text{ ms}$ and $-5 \text{ ms} < \tau_1 < 0$ and the exact shape of the experimental potentiation zone in the quarter $\tau_1 < 0$ and $\tau_2 > 0$ is not clear. Other experimental studies predict a different result for this interaction: in cultured hippocampal neurons (Wang et al., 2005), 1pre-2post interaction with $\tau_1 < 0$ and $0 < \tau_2 < 25 \text{ ms}$ should lead to potentiation, which is in this case completely coherent with our results. We find that 2pre-1post triplets (+10,-10) induce no significant synaptic change, whereas 1pre-2post triplets (-10,+10) induce LTP. 2pre-1post triplets with $0 < \tau_1 < 25 \text{ ms}$ and $\tau_2 < 0$ leads to no plasticity or weak LTP. (Fig. 11C, upper diagram). In contrast, 1pre-2post triplets with $0 < \tau_2 < 25 \text{ ms}$ and $\tau_1 < 0$ leads to much stronger LTP (Fig. 11C, bottom diagram). This means that, on one hand, when depression is followed by potentiation, potentiation dominates. On the other hand, when depression is followed by potentiation, potentiation and depression cancels. These results are coherent with experimental results (Wang et al., 2005). With too short time intervals, the model do not reproduce so well the experimental results: (+15,-5) triplets induce weak LTP (cfr. Fig. 12) (in experiments, nothing) while (-15,+5) triplets induce LTP, as in experiments. In the model, the spine is far from the soma, and the propagation time of the BAP

could explain some of the discrepancies of the model at very short time intervals. The influence of the length and the position of the spine on the shape of the STDP curve needs a complete and in-depth study. This issue will be treated in future work.

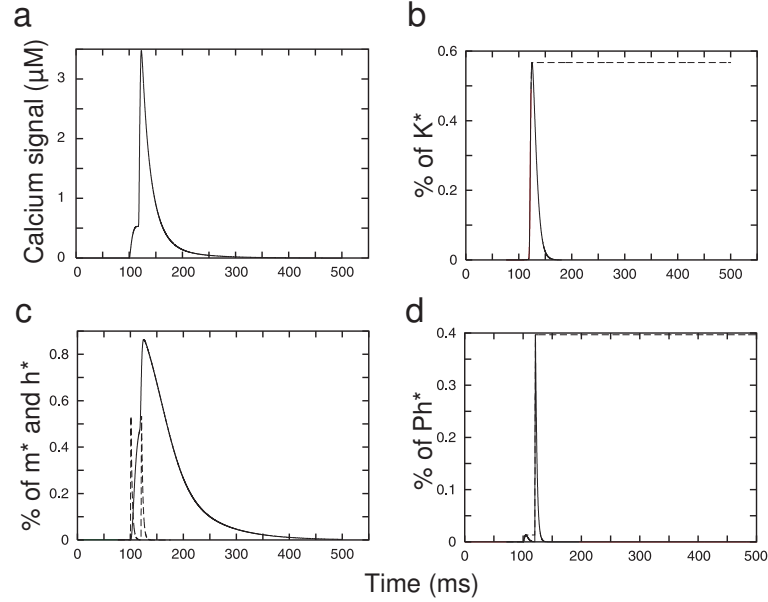


Fig. 12. Mechanism underlying triplet interactions in the biophysical model. Example of a triplet with one presynaptic event and two postsynaptic events, with $\tau_1 = -15$ ms and $\tau_2 = 5$ ms (see Fig. 11A for the definition of τ_1 and τ_2). Same representation as in Fig. 2: a: calcium concentration in the spine; b: fraction of activated LTP enzyme (dashed trace is the maximum of this function, proportional to LTP); c: fraction of activated *m*-enzyme (continuous) and *h*-enzyme (dashed); d: fraction of activated LTD enzyme (dashed trace is the maximum of this function, proportional to LTD).

According to Wang et al. (2005) results, in the presence of a CamKII blocker ($ak=0$ in the model), both triplets result in depression. Pre-post pairing resulted in no significant LTD. In the presence of a blocker of calcineurin ($am=0$ in our model) both triplets induced LTP and post-pre pairing resulted in neither LTP or LTD. Our model leads to the same results in all of these cases. These results show that the independence of the two pathways (potentiation and depression) introduced in the model is a biologically relevant characteristic, when compared to experimental results.

Even if some experimental results are well reproduced, the biophysical model has several limitations. First, it contains many parameters, such as the activation rate constants of the enzymes, which are unknown and difficult to measure. Their values were adjusted here in an ad-hoc fashion, in order to obtain STDP curves consistent with experimental measurements. Second, it does not handle the saturation of the synaptic weight, after a certain number of pairings. A mechanism could certainly have been inserted in the model (for example by limiting the total number of receptors), but would complicate it. Third, the complexity of the model makes it hard to manipulate, even at the level of a single spine, so its application for network-level models is problematic. This last point was the main reason for developing a simplified model.

The simplified model is computationally efficient, but also has limitations. The main limit is the explicit incorporation of spike efficacy factors ($\epsilon_{i,j}$) in order to account for multiple spike interactions such as found in triplet experiments (Fig. 11D). Although the biological meaning of spike efficacies is not clear, this model has the merit of being extremely fast to compute because the corresponding equations are solvable analytically. This model should therefore find applications in network simulations in which several thousand synapses could incorporate STDP mechanisms at reasonable computational expense.

Several important points need to be explored by further work. More experiments are needed, in various conditions, to confirm the generality of STDP rules. For the moment, STDP results are mostly based on *in vitro* experiments in young

animals or in organotypic cultures, although quantitative reexamination of the applicability of STDP *in vivo* is under way in adult primary visual cortex (René et al., 2003) and barrel cortex (Shulz et al., 2004). For example, experimental data are sometimes conflicting about triplet interactions (cfr. above, Froemke and Dan, 2002 versus Wang et al., 2005). More experiments are needed to conclude if the discrepancy is due to a difference in the system (cortical slices versus cultured hippocampal neurons) or not. In contrast, many *in vivo* experiments are consistent with the BCM theory and the calcium hypothesis (Frégnac and Shulz, 1999; reviewed in Frégnac, 2002). A comprehensive biophysical model is still to be sought, to obtain a common framework relating BCM, STDP rules and calcium signals (for simplified models relating BCM and STDP, without calcium, see Izhikevich and Desai, 2003).

6. Acknowledgments

Research supported by CNRS, HFSP, the French Government (ACI "synaptic plasticity and functional adaptation") and the European Community (IST 2001-34712). Three related papers (Rubin et al., 2005; Wang et al., 2005; Shouval and Kalantzis, 2005) appeared after this study was done. We thank the referees for drawing our attention towards them.

7. References

- Allbritton N.L., Meyer T. and Stryer L. (1992) Range of messenger action of calcium ion and inositol 1,4,5-triphosphate, *Science* 258, 1812-1815.
- Artola A., Brocher S. and Singer W. (1990) Different voltage-dependent thresholds for inducing long-term depression and long-term potentiation in slices of rat visual cortex. *Nature* 347, 69-72.
- Artola A. and Singer W. (1993) Long-term depression of excitatory synaptic transmission and its relationship to long-term potentiation, *Trends Neurosci.* 16, 480-487.
- Bear M.F. (1995) Mechanism for a sliding synaptic modification threshold, *Neuron* 15, 1-4.
- Bear M.F., Cooper L.N. and Ebner F.F. (1987) A physiological basis for a theory of synapse modification, *Science* 237, 42-48.
- Bell C.C., Han V.Z., Sugawara Y. and Grant K. (1997) Synaptic plasticity in a cerebellum-like structure depends on temporal order, *Nature* 387, 278-81.
- Bi G.Q. and Poo M.M. (1998) Synaptic modifications in cultured hippocampal neurons dependence on spike timing, synaptic strength, and postsynaptic cell type, *J. Neurosci.* 18, 10464-10472.
- Bienenstock E.L., Cooper L.N. and Munro P.W. (1982) Theory for the development of neuron selectivity: orientation specificity and binocular interaction in visual cortex. *J. Neurosci.* 2, 32-48.
- Boettiger C.A. and Doupe A.J., Developmentally restricted synaptic plasticity in a songbird nucleus required for song learning, *Neuron* 31, 809-818.
- Brocher S., Artola A. and Singer W. (1992) Intracellular injection of Ca²⁺ chelators blocks induction of long-term depression in rat visual cortex, *Proc. Natl. Acad. Sci. USA* 89, 123-127.
- Carmignoto G. and Vicini S. (1992) Activity-dependent decrease in NMDA receptor responses during development of the visual cortex, *Science* 258, 1007-1011.
- Castellani G.C., Quinlan E.M., Cooper L.N. and Shouval H.Z. (2001) A biophysical model of bidirectional synaptic plasticity: dependence on AMPA and NMDA receptors. *Proc. Natl. Acad. Sci. USA* 98, 12772-12777.

- Colbran R.J. (2004) Protein phosphatase and calcium/calmodulin-dependent protein kinase II-dependent synaptic plasticity, *J. Neurosci.* 24, 8404-8409.
- Cormier R.J., Greenwood A.C. and Connor J.A. (2001) Bidirectional synaptic plasticity correlated with the magnitude of dendritic calcium transients above a threshold, *J Neurophysiol.* 85, 399-406.
- Cummings J.A., Mulkey R.M., Nicoll R.A. and Malenka R.C. (1996) Ca²⁺ signaling requirements for long-term depression in the hippocampus, *Neuron* 16, 825-833.
- D'Alcantara P., Schiffmann S.N. and Swillens S. (2003) Bidirectional synaptic plasticity as a consequence of interdependent Ca²⁺-controlled phosphorylation and dephosphorylation pathways, *Eur. J. Neurosci.* 17, 2521-2528.
- Destexhe A., Babloyantz A. and Sejnowski T.J. (1993) Ionic mechanisms for intrinsic slow oscillations in thalamic relay neurons, *Biophys. J.* 65, 1538-1552.
- Destexhe A., Mainen Z.F. and Sejnowski T.J. (1994) An efficient method for computing synaptic conductances based on a kinetic model of receptor binding, *Neural Comput.* 6, 10-14.
- Destexhe A., Mainen Z.F., Sejnowski T.J. (1998) Kinetic models of synaptic transmission. In: *Methods In Neuronal Modeling*, Edited by Koch, C. and Segev, I. MIT Press, Cambridge, MA, pp. 1-26.
- Dudek S.M. and Bear M.F. (1992) Homosynaptic long-term depression in area CA1 of hippocampus and effects of N-methyl-D-aspartate receptor blockade, *Proc. Natl. Acad. Sci. USA*, 89, 4363-4367.
- Eggermont J.J. (1991) Neuronal pair and triplet interactions in the auditory midbrain of the leopard frog. *J. Neurophysiol.* 66, 1549-1563.
- Feldman D.E. (2000) Timing-based LTP and LTD at vertical inputs to layer II/III pyramidal cells in rat barrel cortex, *Neuron* 27, 45-56.
- Feldmeyer D., Lubke J., Silver R.A. and Sakmann B. (2002) Synaptic connections between layer 4 spiny neurone-layer 2/3 pyramidal cell pairs in juvenile rat barrel cortex: physiology and anatomy of interlaminar signaling within a cortical column. *J. Physiol.* 538, 803-822.
- Frégnac Y. (2002) Hebbian synaptic plasticity. In: *Handbook of Brain Theory and Neural Networks* (edited by Arbib, M.A., MIT Press, Cambridge MA), pp. 512-522.
- Frégnac Y. and Shulz D. (1999) Activity-dependent regulation of receptive field properties of cat area 17 by supervised Hebbian learning. *J. Neurobiol.*, 41, 69-82.
- Frome R.C. and Dan Y. (2002) Spike-Timing-dependent synaptic modification induced by natural spike trains. *Nature*, 416, 433-438.
- Gold J.I. and Bear M.F. (1994) A model of dendritic spine Ca²⁺ concentration exploring possible bases for a sliding synaptic modification threshold. *Proc. Natl. Acad. Sci. USA*, 91, 3941-3945.
- Goldman D.E. (1943) Potential, impedance, and rectification in membranes, *J. Gen. Physiol.* 27, 37-60.
- Gutig, R., Aharonov, R., Rotter, S. and Sompolinsky, H. (2003) Learning input correlations through nonlinear temporally asymmetric Hebbian plasticity. *J. Neurosci.* 23, 3697-3714.
- Hanson P.I. and Schulman H. (1992) Neuronal Ca²⁺/calmodulin-dependent protein kinases, *Annu. Rev. Biochem.* 61, 559-601.
- Harris K.M. and Kater S.B. (1994) Dendritic spines : cellular specializations imparting both stability and flexibility to synaptic function, *Annu. Neurosci.* 17, 341-371.

- Hines M.L. and Carnevale N.T. (1997) The NEURON simulation environment, *Neural Comput.* 9, 1179-1209.
- Hodgkin A.L. and Katz B. (1949) The effect of sodium ions on the electrical activity of the giant axon of the squid, *J. Physiol. (London)* 108, 37-77.
- Holthoff K., Tsay D. and Yuste R., (2002) Calcium dynamics of spines depend on their dendritic location, *Neuron* 33, 425-437.
- Izhikevich E.M. and Desai N.S. (2003) Relating STDP to BCM, *Neural Computation* 15, 1511-1523.
- Jahr C.E. and Stevens C.F. (1993) Voltage dependence of NMDA-activated macroscopic conductances predicted by single-channel kinetics. *J. Neurosci.* 9, 3178-3182.
- Karmarkar U.R. and Buonomano D.V. (2002) A model of spike-timing dependent plasticity: one or two coincidence detectors? *J. Neurophysiol.* 88, 507-513.
- Kirkwood A. and Bear M.F. (1994) Homosynaptic long-term depression in the visual cortex, *J. Neurosci.* 14, 3404-3412.
- Levy W. B., and Desmond N. L. (1985) The rules of elemental synaptic plasticity. In: *Modifications, Neuron selectivity and Nervous System Organization*, W. B. Levy, J. Anderson, and S. Lehmkhule, eds. (Erlbaum, New Jersey), pp. 105-121.
- Levy, W.B and Steward, O. (1983) Temporal contiguity requirements for long-term associative potentiation/depression in the hippocampus, *Neuroscience* 8, 791-797.
- Lisman J.E. (1985) A mechanism for memory storage insensitive to molecular turnover: a bistable autophosphorylating kinase, *Proc. Natl. Acad. Sci. USA* 82, 3055-3057.
- Lisman J.E. (1989) A mechanism for the Hebb and than anti-Hebb processes underlying learning and memory, *Proc. Natl. Acad. Sci. USA* 86, 9574-9578.
- Liu L., Wong T.P., Pozza M.F., Lingenhoehl K., Wang Y., Sheng M., Auberson Y.P. and Wang Y.T. (2004) Role of NMDA receptor subtypes in governing the direction of hippocampal synaptic plasticity, *Science* 304, 1021-1024.
- Lynch G., Larson J., Kelso S., Barrionuevo G. and Schottler, F. (1983) Intracellular injections of EGTA block induction of hippocampal long-term potentiation, *Nature* 305, 719-721.
- Magee J.C. and Johnston D.A. (1997) A synaptically controlled, associative signal for Hebbian plasticity in hippocampal neurons, *Science* 275, 209-213.
- Mainen Z.F. and Sejnowski T. J. (1996) Influence of dendritic structure on firing pattern in model neocortical neurons, *Nature* 382, 363-366.
- Malenka R.C., Kauer J.A., Zucker R.S. and Nicoll R.A. (1988) Postsynaptic calcium is sufficient for potentiation of hippocampal synaptic transmission, *Science* 242, 81-84.
- Markram H., Helm P.J. and Sakmann, B. (1995) Dendritic calcium transients evoked by single back-propagating action potentials in rat neocortical pyramidal neurons, *J. Physiol.* 485, 1-20.
- Markram H., Lubke J., Frotscher M. and Sakmann B. (1997) Regulation of synaptic efficacy by coincidence of postsynaptic Aps and EPSPs, *Science*, 265, 774-777.
- Massey P.V., Johnson B.E., Moulton P.R., Auberson Y.P., Brown M.W., Molnar E., Collingridge G.L. and Bashir Z.I. (2004) Differential roles of NR2A and NR2B-containing NMDA receptors in cortical long-term potentiation and long-term depression. *J. Neurosci.* 24, 7821-7828.

- Miller S.G. and Kennedy M.B. (1986) Regulation of brain type II Ca^{2+} /calmodulin-dependent protein kinase by autophosphorylation: a Ca^{2+} -triggered molecular switch, *Cell* 44, 861-870.
- Mulkey R.M. and Malenka R.C. (1992) Mechanisms underlying induction of homosynaptic long-term depression in area CA1 of the hippocampus, *Neuron* 9, 967-975.
- Nase G., Weishaupt J., Stern P., Singer W. and Monyer H. (1999) Genetic and epigenetic regulation of NMDA receptor expression in the rat visual cortex. *Eur. J. Neurosci.* 11, 24320-24326.
- Neveu D. and Zucker R.S., (1996) Postsynaptic levels of $[\text{Ca}^{2+}]_i$ needed to trigger LTD and LTP, *Neuron* 16, 619-629.
- Nishiyama M., Hong K. and Mikoshiba K. (2000). Calcium stores regulate the polarity and input specificity of synaptic modification, *Nature* 408, 584-588.
- Oliet S., Malenka R.C. and Nicoll R.A. (1997) Two distinct forms of long-term depression coexist in CA1 hippocampal pyramidal cells, *Neuron* 18, 969-982.
- Quinlan E.M., Olstein D.H. and Bear M.F. (1999) Bidirectional, experience-dependent regulation of N-methyl-D-aspartate receptor subunit composition in the rat visual cortex during postnatal development, *Proc. Natl. Acad. Sci. USA*, 96, 12876-12880.
- René A., Huguet N., Pananceau M. and Frégnac, Y. (2003) An in vivo generalization of Hebbian plasticity rules in adult visual cortex to multiple pre-post synaptic activity correlation, *Soc. Neurosci. Abstracts*, 29, 266-17
- Rubin J.E., Gerkin R.C., Bi G.-Q. and Chow C.C. (2005) Calcium time course as a signal for spike-timing-dependent plasticity, *J. Neurophysiol.* 93, 2600-2613.
- Sabatini, B.L. Oertner T.G. and Svoboda K. (2002). The life cycle of Ca^{2+} ions in dendritic spines, *Neuron* 33, 439-452.
- Sabatini B.L. and Svoboda K. (2000) Analysis of calcium channels in single spines using optical fluctuation analysis, *Nature* 406, 589-593.
- Senn W., Markram H. and Tsodyks M. (2001) An algorithm for modifying neurotransmitter release probability based on pre- and postsynaptic spike timing, *Neural Comput.* 13, 35-67.
- Shouval H.Z., Bear M.F. and Cooper L.N. (2002) A unified model of NMDA receptor-dependent bidirectional synaptic plasticity, *Proc. Natl. Acad. Sci. USA* 99, 10831-10836.
- Shouval H.Z. and Kalantzis, G. (2005) Stochastic properties of synaptic transmission affect the shape of spike time-dependent plasticity curves, *J. Neurophysiol.*, 93, 1069-1073.
- Shulz D.E., Brasier D.J. and Feldman D.E. (2004) Spike-timing dependent plasticity investigated using Whole-cell recording in rat somatosensory cortex (S1) in vivo, *Soc. Neurosci. Abstracts*, 30,.
- Sjostrom J., Turrigiano G.G. and Nelson S.B. (2001) Rate, timing, and cooperativity jointly determine cortical synaptic plasticity, *Neuron* 32, 1149-1164.
- Song S., Miller K.D., and Abbott L.F. (2000) Competitive Hebbian learning through spike-timing-dependent synaptic plasticity, *Nat. Neurosci.* 3, 919-926.
- Stuart G.J. and Hausser M. (2001) Dendritic coincidence detection of EPSPs and action potentials, *Nat. Neurosci.* 4, 63-71.
- van Rossum, M.C., Bi, G.Q. and Turrigiano G.G. (2000) Stable Hebbian learning from spike timing-dependent plasticity. *J. Neurosci.* 20, 8812-8821.

- Wang H.X., Gerkin R.C., Nauen D.W., Bi G.Q. (2005) Coactivation and timing-dependent integration of synaptic potentiation and depression, *Nat. Neurosci.* 2, 187-193.
- Yang S.N., Tang Y.G. and Zucker R.S., (1999) Selective induction of LTP and LTD by postsynaptic $[Ca^{2+}]_i$ elevation, *J. Neurophysiol.* 81, 781-787.
- Yasuda H. and Tsumoto T. (1996) Long-term depression in rat visual cortex is associated with a lower rise of postsynaptic calcium than long-term potentiation, *Neurosci. Res.* 24, 265-274.
- Yuste R. and Denk W. (1995) Dendritic spines as basic functional units of neuronal integration, *Nature* 375, 682-684.
- Zhabotinsky A. M. (2000) Bistability in the Ca^{2+} /Calmodulin-dependent protein kinase-phosphatase system, *Biophys. J.* 79, 2211-2221.
- Zucker R.S. (1999) Calcium- and activity-dependent synaptic plasticity, *Curr. Opin. Neurobiol.* 9, 305-313.